19th Australasian Fluid Mechanics Conference
Melbourne, Australia
8-11 December 2014

Inertial Effects on the Capture of Particles in Aquatic Systems

A. Espinosa-Gayosso[1,2], M. Ghisalberti[1], G. N. Ivey[1,2] and N. L. Jones[1,2]

[1]School of Civil, Environmental and Mining Engineering
University of Western Australia, Crawley, WA 6009, Australia

[2]UWA Oceans Institute
University of Western Australia, Crawley, WA 6009, Australia

Abstract

Particle capture, whereby suspended particles contact and adhere to a solid surface (a 'collector'), is an important mechanism for a range of aquatic environmental processes. Although particle inertia is often ignored in the analysis of particle capture in aquatic systems, inertial effects can become important under certain conditions. In this paper, we use a numerical analysis of Lagrangian trajectories of aquatic-type particles (where the ratio of particle density to fluid density is close to one) to quantify the influence of inertia on particle capture in a parameter space relevant to aquatic systems. Our analysis shows that inertia can not only augment capture efficiency but also diminish it, and that inertial effects appear well before the critical Stokes number is reached. The role of particle inertia is maximised at Stokes numbers above the critical value and can result in as much as a six-fold increase in the capture of particles with a density similar to that of suspended sediment.

Introduction

The term 'particle capture' refers to the physical process by which suspended particles come into contact with a solid structure ('collector') and adhere to the collector's surface, as shown in figure 1. One important example of particle capture in aquatic systems is the adhesion of particles to aquatic vegetation surfaces, a phenomenon which defines the filtration and water purification capacity of vegetated wetlands. Particle capture is also of significant ecological importance in marine ecosystems; in particular, it controls the efficiency of seagrass pollination, suspension feeding (of e.g. corals), and larval settlement. The effects of particle inertia can become important under certain conditions but, despite their relevance to ecological function, these effects have not yet been analysed in a parameter space relevant to aquatic environments.

For simplicity, collectors such as vegetation stems or the capturing filaments of suspension feeders are often modelled as cylinders and particles as spheres. The capture efficiency (η) of a cylindrical collector can be defined as the ratio of the number of particles captured (N_c) to the number of particles whose centres would have passed through the space occupied by the collector were it not present in the flow (N_a):

$$\eta = \frac{N_c}{N_a}. \tag{1}$$

In general, capture efficiency depends on four parameters,

$$\eta = \eta(r_p, \rho^+, Re, Pe), \tag{2}$$

where r_p is the particle size ratio, ρ^+ is the particle density ratio, Re is the Reynolds number of the collector and Pe is the Péclet number for particle transport. The definition of each of these parameters is as follows:

$$r_p = \frac{D_p}{D} \equiv \frac{R_p}{R}, \tag{3}$$

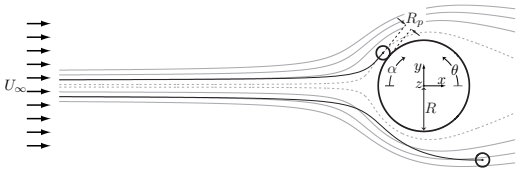

Figure 1: Steady flow conceptualisation of particle capture by inertial impaction. As the trajectories of particles influenced by inertia (indicated in black) do not coincide with the flow streamlines (indicated in grey), the capture efficiency of particles influenced by inertia (η_{IN}) differs from the direct interception value (η_{DI}). Here we consider perfect particle-collector adhesion, such that all particles are assumed to be captured when they contact the cylinder surface.

$$\rho^+ = \frac{\rho_p}{\rho}, \tag{4}$$

$$Re = \frac{\rho U_\infty D}{\mu}, \tag{5}$$

$$Pe = \frac{U_\infty D}{\Gamma_p}, \tag{6}$$

where D_p and R_p are the particle diameter and radius, D and R are the collector diameter and radius, ρ_p is the particle density, ρ is the fluid density, U_∞ is the uniform upstream fluid velocity, μ is the fluid viscosity and Γ_p is the particle diffusivity. However, the parameter typically chosen to represent the importance of particle inertia is the Stokes number (St) [7], as this non-dimensional group appears naturally in the drag term of the particle momentum equation for aerosols ($\rho^+ \gg 1$). The definition of St incorporates r_p, ρ^+ and Re:

$$St = \frac{\rho_p D_p^2 U_\infty}{9\mu D} = \frac{\rho^+ r_p^2 Re}{9}. \tag{7}$$

The values of these parameters define the relative importance of three different mechanisms of particle capture [7]: (i) inertial impaction, where particle inertia causes deviation from fluid pathlines (streamlines in steady flow), and contact with the collector (figure 1), (ii) diffusional deposition, where particle-collector contact is driven by random motions (such as Brownian motion) and (iii) direct interception, where particle centres follow the pathlines and contact is made due to the finite particle size .

As discussed by Espinosa *et al.* [4, 5], direct interception has been recognized as an important capture mechanism in aquatic systems. When compared with direct interception, inertial and diffusive effects on particle capture are typically neglected in the aquatic systems of interest, due to the low Stokes numbers (St) and high Péclet numbers (Pe) of suspended particles, respectively. We have recently obtained accurate analytical and graphical tools for estimating particle capture by direct

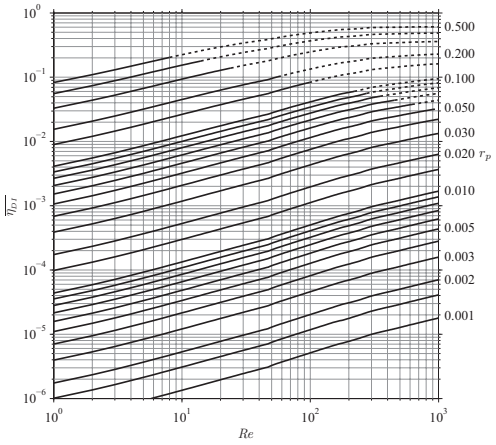

Figure 2: The efficiency of particle capture by direct interception (η_{DI}), which increases with Reynolds number (Re) and particle size ratio (r_p) (from [5]).

interception covering a range of particle sizes ($0 < r_p \leqslant 1.5$) and flow conditions (from creeping flow up to intermediate Reynolds numbers, i.e. $0 < Re \leqslant 1000$) which are relevant to aquatic systems (figure 2). In the present study we extend this work by considering the effects of particle inertia in the absence of diffusive effects.

The capture efficiency for particles with inertia (η_{IN}) differs from the direct interception value (η_{DI}) for the same r_p and Re, as their dynamics also depend on the particle density ratio (ρ^+). However, in the limit of high particle inertia, particles are not influenced by the flow field and travel in straight-line trajectories in the streamwise direction. In this limit, the capture efficiency is therefore given by

$$\eta_{IN,max} = 1 + r_p. \tag{8}$$

There has been considerable analytical and experimental research into the effects of inertia on the capture of aerosols ($\rho^+ \gg 1$) (see, e.g., [6, 7]). However, such studies are not applicable to aquatic systems as they are characterised by one or more of the following conditions: (i) very high particle density ratios ($\rho^+ \gg 1$), (ii) a focus on a narrow range of flow conditions (usually inviscid or creeping flow fields, which can be described analytically), (iii) neglect of the finite particle size ($r_p \ll 1$), and/or (iv) a focus on a range of St where inertial impaction is entirely dominant. In aquatic systems, the particles of interest have a density similar to that of water ($\rho^+ \sim O(1)$), the flow conditions cover a wide range of Re ($0 < Re \lesssim 1000$), particle sizes can be of the order of the collector diameter ($r_p \sim O(1)$), and St is in a range where both direct interception and inertial impaction may be dominant. The effects of inertia on particle capture have yet to be described in a parameter space relevant to aquatic systems.

Due to the low particle density ratio ($\rho^+ \sim O(1)$), the equations of motion for aquatic-type particles cannot be simplified to the equations commonly used for aerosols [1]; the dynamics of aquatic-type particles are very different to those of aerosols in a wide range of flow conditions [9]. Furthermore, when particles are neutrally buoyant ($\rho^+ = 1$), inertial effects are almost completely suppressed; while the behaviour of such particles is very close to that of a perfect tracer, it can differ in zones with large fluid velocity gradients [1]. Here we use a numerical scheme to evaluate the effects of inertia on the capture efficiency of aquatic-type particles by calculating their Lagrangian trajectories in mean flow fields (with time and axial averages obtained from direct numerical simulation (DNS)). We compare the capture efficiencies of particles with inertia (η_{IN}) to those when inertia is not considered (i.e. pure direct interception, [4, 5]) and discuss the reasons behind the differing behaviours.

Basic Equations of Motion and Numerical Methods

Equations of fluid motion

The governing equations are the continuity and Navier-Stokes equations for incompressible flow. Here they are non-dimensionalized with the uniform free-stream velocity U_∞ as the velocity scale, and the radius of the collector R as the length scale:

$$\nabla \cdot u = 0 \tag{9}$$

and

$$\frac{\partial u}{\partial t} + (\nabla u)u = -\nabla p + \frac{2}{Re}\nabla^2 u, \tag{10}$$

where u is the non-dimensional fluid velocity vector, p is the non-dimensional pressure, t is the non-dimensional time and Re is the Reynolds number based on the diameter of the collector, as defined by (5).

Equations of particle motion

Here we consider the influence of the fluid flow on particle motion but neglect the influence of the particles on the fluid motion. Particle-particle interaction effects are also neglected. The Lagrangian equations for each particle [1] can be written in non-dimensional form as:

$$\frac{dx_c}{dt} = v_c \tag{11}$$

$$\rho^+ \frac{dv_c}{dt} = \frac{Du_c}{Dt} - \frac{9}{r_p^2 Re}(v_c - u_c) - \frac{1}{2}\left(\frac{dv_c}{dt} - \frac{Du_c}{Dt}\right) \tag{12}$$

where x_c is the non-dimensional position vector of the centre of the particle, v_c is the non-dimensional velocity of the particle (measured at its centre) and $u_c = u(x = x_c(t), t)$ is the fluid velocity at the position of the particle at any instant (consistent with the assumption that particles do not disturb the fluid); $(v_c - u_c)$ therefore represents the velocity of the particle relative to the fluid. The terms on the right of (12) are the horizontal forces acting on the particle and represent, respectively, the fluid acceleration, the Stokes drag and the added mass effect. As in Babiano *et al.* [1], we are neglecting additional forces due to Faxén corrections and Basset-Boussinesq history. The derivative Du_c/Dt is taken along the path of a fluid element,

$$\frac{Du_c}{Dt} = \frac{\partial u_c}{\partial t} + (\nabla u_c)u_c, \tag{13}$$

while the derivative du_c/dt is taken along the trajectory of the particle,

$$\frac{du_c}{dt} = \frac{\partial u_c}{\partial t} + (\nabla u_c)v_c, \tag{14}$$

so that

$$\frac{Du_c}{Dt} = \frac{du_c}{dt} - (\nabla u_c)(v_c - u_c). \tag{15}$$

The particle momentum equation (12) can then be rewritten as

$$\frac{dv_c}{dt} = -\left(\frac{2\rho^+}{2\rho^+ + 1}\right)\frac{1}{St}(v_c - u_c) + \frac{3}{2\rho^+ + 1}\frac{Du_c}{Dt}. \tag{16}$$

If dealing with aerosols ($\rho^+ \gg 1$), (16) can be further simplified to

$$\frac{dv_c}{dt} = -\frac{1}{St}(v_c - u_c). \tag{17}$$

However, for aquatic systems with $\rho^+ \sim O(1)$, all the terms in (16) must be retained. Following Babiano *et al.* [1], we substitute (15) into (16) and rewrite it in terms of the relative particle velocity to obtain

$$\begin{aligned} \frac{d}{dt}(v_c - u_c) &= -\left(\frac{2\rho^+}{2\rho^+ + 1}\right)\frac{1}{St}(v_c - u_c) \\ &- \frac{3}{2\rho^+ + 1}(\nabla u_c)(v_c - u_c) \\ &- \frac{2(\rho^+ - 1)}{2\rho^+ + 1}\frac{du_c}{dt}. \end{aligned} \tag{18}$$

This form of the momentum equation shows that perfectly neutrally-buoyant particles ($\rho^+ = 1$), for which the last term on the right hand side of (18) disappears, behave as perfect tracers only if the second term (the one containing the fluid velocity gradient) can also be neglected. In that case, after some initial difference between the particle and the fluid velocities, the relative particle velocity would decay exponentially with time [1] and particles would follow fluid paths exactly. But when the fluid velocity gradient is large (as in zones close to stagnation points [1]) or when the particles are not perfectly neutrally-buoyant, the two last terms on the RHS of (18) induce particle dynamics which differ from both those of a perfect tracer and those characterised by the common aerosol simplification (17).

Numerical Methods for Estimating Particle Trajectories

Capture efficiencies and critical Stokes numbers were estimated with a Lagrangian approach by 'seeding' particles within a series of fully-developed flow solutions (obtained from DNS as described in our previous work [4, 5]. Both the fluid velocity and velocity gradient fields were imported into MATLAB®[1] release 2013b, and the particle trajectories calculated within the framework of this numerical tool. When $Re \leqslant 47$, the flow is steady; above this value of Re, the flow is unsteady. However, calculation of particle trajectories in unsteady flow fields is very computationally expensive. Consequently, in this range of higher Re, DNS flow fields were first axially- and time-averaged into mean flow fields before particle trajectories were calculated. For $Re > 180$, at least 50 oscillation cycles of fully-developed flow were used for the averaging in time, as the flow is no longer perfectly time-periodic when three-dimensional vortex shedding is present [8].

For the particle capture estimates, 'clouds' of particles of finite size were seeded into the computational domain upstream of the cylinder with an initial velocity equal to that of the fluid at the particles' initial positions (i.e. $v_c(t=0) = u_c$). For critical Stokes number estimates in viscous flow ($St_{c,\nu}$), a single 'point' particle was seeded on the stagnation streamline for each St tested, and the St was incremented by 0.0001 until a particle was able to reach the stagnation point, following the 'classical' idea of Taylor [10]. In the seeding zone, the fluid velocity was always within 0.01% of the uniform flow condition, i.e. $(u,v,w) \approx (U_\infty, 0, 0)$. Particle trajectories were obtained by integrating (11) and (18) using an algorithm based on the explicit Runge-Kutta (4,5) pair formula of Dormand and Prince [3]. The fluid velocity and the velocity gradient at the particle centre (u_c and ∇u_c) were obtained with a linear piecewise spatial interpolation of the mean DNS fields, which generates continuous fields at any position in the domain. The time-step always satisfied $\Delta t < 0.1\,St$, a requirement for accurate simulation of particle motion [2]. Particles were deemed to be captured when they touched the collector (i.e. when their centre came within one particle radius of the collector surface). Capture efficiency was estimated using equation (1) after all the non-captured particles had exited the domain.

[1] MATLAB® is a registered trade mark of The MathWorks Inc., Natick, Massachusetts, U.S.A.

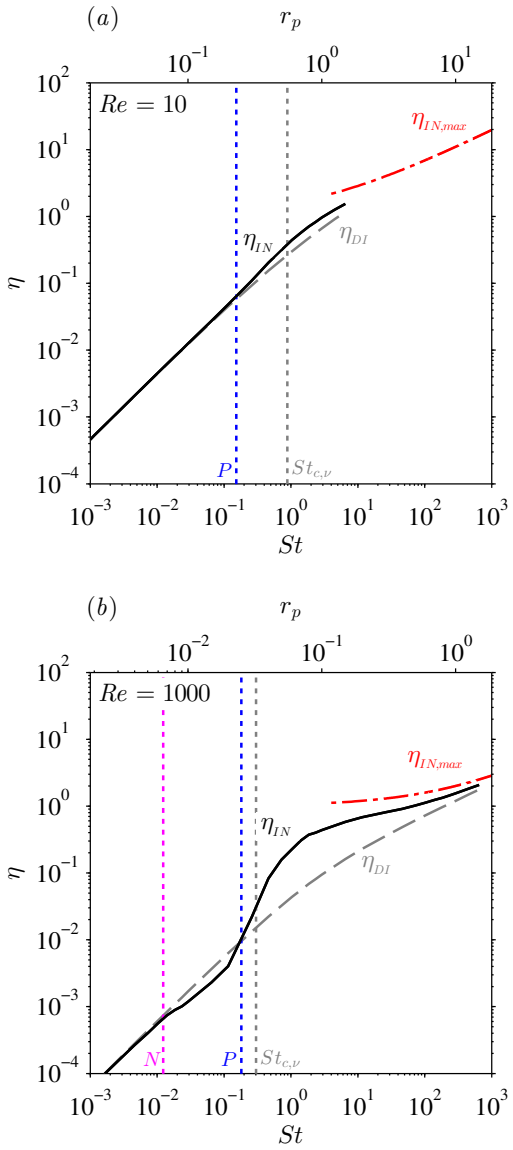

Figure 3: Capture efficiencies considering inertia and finite particle size (η_{IN}) for sediment-type particles ($\rho^+ = 2.6$) as a function of St (or r_p) for (*a*) $Re = 10$ and (*b*) $Re = 1000$.

Inertial Effects on the Efficiency of Capture of Aquatic-type Particles

Here, we describe the effect of inertia on the capture efficiency of aquatic-type particles ($\rho^+ \sim O(1)$) over ranges of Re and St (or r_p) common to aquatic systems. The results are presented in comparison to the capture efficiencies estimated by considering only direct interception [4, 5].

We found neutrally-buoyant particles ($\rho^+ = 1$) follow almost perfectly the trajectories defined by the mean streamlines. The difference of particle capture efficiency compared to that of pure

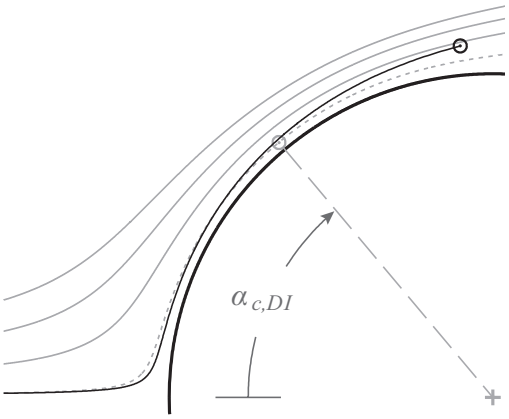

Figure 4: Graphical analysis of the centrifugal drift that induces a reduction in capture efficiency for sediment-type particles with weak inertial influence ($\rho^+ = 2.6$, $St = 0.11$, $r_p = 0.02$, $Re = 1000$). Plot of the trajectory of a particle with weak inertia influence (shown in black) that is released on the limiting streamline for direct interception [4, 5] of particles of that size (shown as a dotted line). The particle with weak inertial influence (shown in black) separates from the limiting streamline, but does not reach the collector and drifts centrifugally, therefore decreasing the capture efficiency with respect to direct interception. The capture position of a neutrally-buoyant particle of the same size (shown in grey) and the maximum angle of capture for direct interception ($\alpha_{c,DI}$) are also indicated.

direct interception is less than 0.1% for $Re \leqslant 1000$ and $r_p \leqslant 1.5$. For the Re tested here, the strength of the velocity gradients is not sufficient to cause particles to deviate from effectively perfect tracer behaviour and only direct interception should thus be considered in this case [4, 5].

For the case of sediment-type particles ($\rho^+ = 2.6$), as expected, inertia increases capture efficiency with increasing St (figure 3); the vertical lines labelled as P in this figure show the points at which the capture efficiency increases by 10% relative to direct interception. Note that this 10% increase occurs before reaching the critical Stokes number for viscous flow $St_{c,\mathrm{V}}$. At the critical Stokes value, the increase in capture efficiency reaches 50% for $Re = 10$ and 100% for $Re = 1000$; the maximum increase induced by inertia is as large as 500% for $Re = 1000$ (figure 3*b*). Aquatic-type particle dynamics differ from those of aerosols, such that the increase of η_{IN} with St does not approach the limit of very high particle inertia ($\eta_{IN,max}$).

Inertia can diminish capture efficiency under certain conditions due to the particle-phase compressibility [6]. In our tests for $\rho^+ = 2.6$ and $Re \gtrsim 100$, inertia initially reduces the capture efficiency relative to direct interception before an increase occurs at higher St; the vertical line labelled as N in figure 3(*b*) shows the St at which the capture efficiency decreases by 10% compared to direct interception. For $Re = 1000$, the reduction occurs in the range $0.001 \lesssim St \lesssim 0.17$, and is as large as 40%. This reduction in capture efficiency occurs as particles drift away from the collector due to centrifugal acceleration [6]. The effect is illustrated in figure 4, which displays the trajectory of a particle with weak inertial influence ($St = 0.11$ and $r_p = 0.02$) which is released on the outer-most streamline that allows capture of neutrally buoyant particles of this size (the limiting streamline for direct interception defined by Espinosa-Gayosso et al. [4, 5]).

Conclusions

For aquatic-type particles, we have used a Lagrangian analysis to estimate the influence of inertia on particle capture. We have shown that the velocity gradients for $Re \leqslant 1000$ are not strong enough to induce significant deviations of neutrally-buoyant particles from a perfect-tracer trajectory, such that the only mechanism of capture for neutrally buoyant particles is direct interception. When the particle density ratio is similar to that of sediment in water, the effects of inertia are two-fold: (i) inertia augments the capture efficiency when the Stokes number is sufficiently large, and (ii) counter-intuitively, inertia can reduce capture for particles with weak inertial influence, i.e., lower St. Inertial effects appear at values of St much lower than the critical value. At the critical Stokes number, the increase in capture efficiency exceeds 50% for $Re > 10$. The impact of particle inertia on capture is maximised when $St > St_{c,\mathrm{V}}$ and can result in as much as a six-fold increase in capture efficiency.

Acknowledgements

A. Espinosa-Gayosso acknowledges the scholarships granted by CONACyT-Banco de México, the Australian Government (IPRS) and The University of Western Australia. The authors are grateful to the iVEC supercomputing facility for the resources granted to this study. Helpful comments from Prof. Fernández de la Mora are gratefully acknowledged. This research was supported by an Australian Research Council Discovery Project (DP35603400)..

References

[1] Babiano, A., Cartwright, J. H. E., Piro, O. and Provenzale, A., Dynamics of a small neutrally buoyant sphere in a fluid and targeting in Hamiltonian systems, *Phys. Rev. Lett.*, **84**, 2000, 5764–5767.

[2] Dorgan, A. J. and Loth, E., Efficient calculation of the history force at finite Reynolds numbers, *Int. J. Multiphas. Flow*, **33**, 2007, 833–848.

[3] Dormand, J. R. and Prince, P. J., A family of embedded Runge-Kutta formulae, *J. Comput. Appl. Math.*, **6**, 1980, 19–26.

[4] Espinosa-Gayosso, A., Ghisalberti, M., Ivey, G. N. and Jones, N. L., Particle capture and low-Reynolds-number flow around a circular cylinder, *J. Fluid Mech.*, **710**, 2012, 362–378.

[5] Espinosa-Gayosso, A., Ghisalberti, M., Ivey, G. N. and Jones, N. L., Particle capture by a circular cylinder in the vortex-shedding regime, *J. Fluid Mech.*, **733**, 2013, 171–188.

[6] Fernandez de la Mora, J., Inertia and interception in the deposition of particles from boundary-layers, *Aerosol Sci. Technol.*, **5**, 1986, 261–286.

[7] Friedlander, S. K., *Smoke, dust and haze. Fundamentals of aerosol dynamics*, Oxford University Press, 2000, 2nd edition.

[8] Henderson, R. D., Nonlinear dynamics and pattern formation in turbulent wake transition, *J. Fluid Mech.*, **352**, 1997, 65–112.

[9] Maxey, M. R., The motion of small spherical particles in a cellular flow field, *Phys. Fluids*, **30**, 1987, 1915–1928.

[10] Taylor, G., Note on possible equipment and technique for experiments on icing on aircraft., *Reports and Memoranda of the Aeronautical Research Committee*.